

Consequence of resonant laser excitation and bi-directional quantum dot nuclear spin polarization

C. Latta¹, A. Hoge¹, Y. Zhao², A. N. Vamivakas², P. M. Alekseyev¹, M. Kroner¹, J. Dreiser¹, I. Carusotto^{1,3}, A. Badolato¹, D. Schuh¹, W. Wegscheider¹, M. Atatüre², and A. Imamoglu¹

¹ Institute of Quantum Electronics, ETH-Zurich, CH-8093 Zurich, Switzerland

² Cavendish Laboratory, University of Cambridge, Cambridge CB3 0HE, UK and

³ BEC-CNR-INFM and Dipartimento di Fisica, Università di Trento, I-38050 Povo, Italy

(Dated: February 21, 2024)

Resonant laser scattering along with photon correlation measurements have established the atom-like character of quantum dots. Here, we present measurements which challenge this identification for a wide range of experimental parameters: the absorption lineshapes that we measure at magnetic fields exceeding 1 Tesla indicate that the nuclear spins polarize by an amount that ensures locking of the quantum dot resonances to the incident laser frequency. In contrast to earlier experiments, this nuclear spin polarization is bi-directional, allowing the electron+nuclear spin system to track the changes in laser frequency dynamically on both sides of the quantum dot resonance. Our measurements reveal that the consequence of the laser excitation and nuclear spin polarization suppresses the fluctuations in the resonant absorption signal. A master equation analysis shows narrowing of the nuclear Overhauser field variance, pointing to potential applications in quantum information processing.

PACS numbers:

A number of ground-breaking experiments have demonstrated fundamental atom-like properties of quantum dots (QD), such as photon antibunching [1] and radiative lifetime limited Lorentzian absorption lineshape [2] of optical transitions. Successive experiments using transport [3] as well as optical spectroscopy [4] however, revealed that the nature of hyperfine interactions in QDs is qualitatively different than that of atoms: coupling of a single electron spin to the mesoscopic ensemble of

10^5 QD nuclear spins results in non-Markovian electron spin decoherence [5] and presents a major drawback for applications in quantum information science. Nevertheless, it is still customary to refer to QDs as artificial atoms; i.e. two level emitters with an unconventional dephasing mechanism. Here, we present resonant absorption experiments demonstrating that for a wide range of system parameters, such as the gate voltage, the length of the tunnel barrier that separates the QDs from the back contact and the external magnetic field, it is impossible to isolate the optical excitations of QD electronic states from a strong influence of nuclear spin physics. We determine that the striking locking effect of any QD transition to an incident near-resonant laser, which we refer to as dragging, is associated with dynamic nuclear spin polarization (DNSP); in stark contrast to previous experiments [6, 7, 8, 9, 10, 11, 12] the relevant nuclear spin polarization is bi-directional and its orientation is determined simply by the sign of the excitation laser detuning. We find that fluctuations in the QD transition energy, either naturally occurring [2] or introduced by externally modulating the Stark field, are suppressed when the laser and the QD resonances are locked. We also find that when the exchange interaction between the confined QD electron and the nearby electron Fermi-sea that leads to spin- $\uparrow\downarrow$ co-tunneling [13] is sufficiently strong, it can

suppress the consequence of laser and QD transition energies by inducing fast nuclear spin depolarization [14].

Locking of quantum dot resonances to an incident laser

For a single-electron charged QD, the elementary optical excitations lead to the formation of trion states (X) which are tagged by the angular momentum projection (pseudo-spin) of the optically generated heavy-hole (Fig. 1A). In the absence of an external magnetic field ($B_{\text{ext}} = 0$ T), the absorption lineshape associated with these optical excitations are Lorentzian (Fig. 1B), with a linewidth $\sim 2\Gamma$; here, Γ is the spontaneous emission rate of the trion state. For $B_{\text{ext}} > 100$ mT, the coherent coupling between the (ground) electronic spin states induced by the transverse component of the (quasi-static) nuclear Overhauser field is suppressed [15]: in this limit, the optical excitations of the QD can be considered as forming two weakly coupled two-level systems (Fig. 1A), where the blue (red) trion transition is associated with a QD electron initially in state $|j_z\rangle$ ($|j_z+1\rangle$). Figure 1C shows absorption measurements carried out at $B_{\text{ext}} = 4.5$ T when the laser field with frequency ω_L is tuned across the blue-trion resonance (transition energy $\sim \omega_X$). For a laser that is tuned from an initial blue-detuning to a small red-detuning with respect to the QD resonance (red line in Fig. 1C), we find that the absorption is abruptly turned on when we reach $\omega_L = \omega_X + 2\Gamma$; the absorption strength then remains essentially fixed at its maximal value until we reach $\omega_L = \omega_X + 7\Gamma$, where it abruptly goes to zero. A laser scan in the opposite direction (blue line) shows a complementary picture with the trion absorption strength remaining close to its peak value for laser frequencies that are blue detuned from the bare trion resonance by as much as 7Γ . The absorption

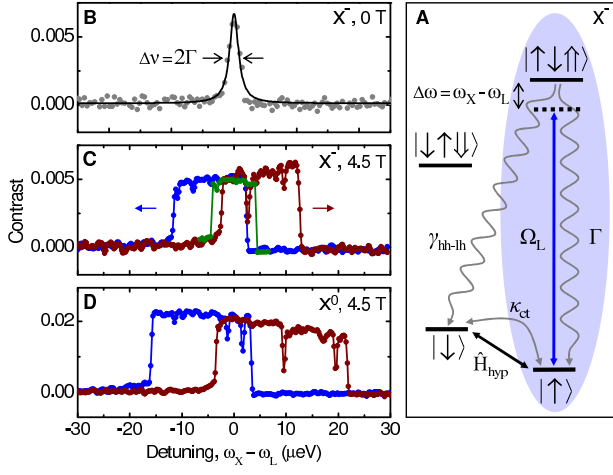


Figure 1: (A) Dragging of quantum dot resonances. Energy-level diagram of a single-electron charged quantum dot: external magnetic field enables spin-selective excitation of Zeeman split trion (X^\pm) states. Right-hand circularly polarized laser with Rabi frequency Ω_L (blue arrow) and detuning $\Delta\omega = \omega_X - \omega_L$ couples the higher energy Zeeman branch between the spin-up electron ground state $| \downarrow \uparrow \downarrow \rangle$ and the trion state $| \uparrow \uparrow \uparrow \rangle$. The relevant decoherence processes (radiative decay Γ , co-tunneling κ_{ct} and heavy-hole/light-hole mixing γ_{hh-lh}) are indicated by grey arrows. (B), (C) Trion absorption spectra at zero magnetic field (Lorentzian fit with a linewidth of 2 μeV) and at 4.5 T, respectively. For magnetic fields exceeding 1 T, the on-resonance scattering is maintained over many natural linewidths to both sides of the bare resonance depending. Red (blue) spectra show data obtained by tuning the laser from an initial blue (red) to a final red (blue) detuning from the quantum dot resonance. The green trace shows the energy range over which resonant absorption is recovered in fixed laser detuning experiments (see Figure 3C). (D) The dragging effect is even more prominent in the absorption spectra of the blue Zeeman branch of the neutral exciton X^0 . In all experiments, the temperature was 4.2 K.

scans of Fig. 1C show that the trion resonance locks on to the laser frequency and can be dragged to either higher or lower energies by tuning the laser frequency, provided that the scan frequency-step size is small. We observe this dragging effect for a wide range of laser Rabi frequencies Ω_L ranging from 0.3 to 3. We also emphasize that dragging is not a simple line-broadening effect: the area of the absorption curve is an order of magnitude larger than its $B_{\text{ext}} = 0$ T counterpart.

It is well known that the optical response of a neutral QD for $B_{\text{ext}} < 1$ T is qualitatively different, owing to the role played by electron-hole exchange interaction [16]. To assess the generality of the dragging phenomenon, we investigated the response of a neutral QD for $B_{\text{ext}} = 2$ T: despite an energy level diagram that is substantially different than that of a single-electron charged QD, the bright exciton transitions of a neutral QD exhibit absorption lineshapes (Fig. 1D) that are qualitatively similar to that of a trion. In fact, we observe that typical dragging widths for neutral QD exciton transitions are

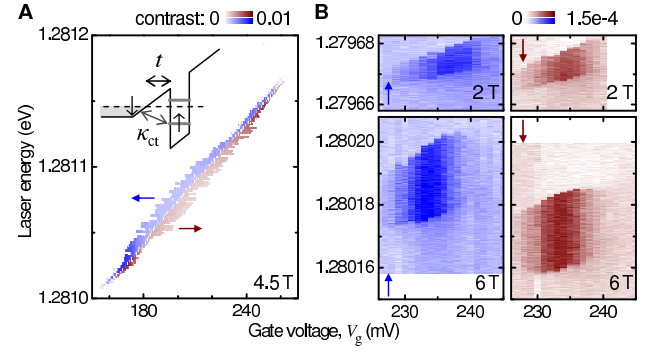


Figure 2: Dependence of dragging on system parameters. Two dimensional absorption maps of the blue trion Zeeman branch as a function of gate voltage and laser energy. Red (blue) arrows indicate the scan direction with decreasing (increasing) laser detuning $\Delta\omega = \omega_X - \omega_L$. (A) Absorption map recorded at 4.5 T for a quantum dot in sample A with a 25 nm tunneling barrier: the data was obtained by keeping the laser energy fixed and scanning the gate voltage. The inset illustrates the exchange coupling to the Fermi reservoir that flips the quantum dot electron spin via co-tunneling events. The co-tunneling rate is minimum in the center and maximum at the edges of the stability plateau; the dragging width scales inversely with the co-tunneling rate κ_{ct} . (B) Absorption maps of a quantum dot in sample B with a 43 nm tunneling barrier that were obtained by scanning the laser at a fixed gate voltage in external magnetic fields of 2 T (upper panel) and 6 T (lower panel). Finite absorption contrast is restricted to the edge of the single-electron charging plateau due to electron spin pumping. The set of data is complementary to (A) and shows that dragging is independent of whether the laser or the gate voltage is scanned. The dragging width increases sub-linearly with increasing strength of the external magnetic field.

significantly larger than that of trion transitions [27].

Further insight into the locking phenomenon depicted in Figs. 1C-D can be gained by studying its dependence on basic system parameters. Figure 2 shows the two-dimensional (2D) map of resonant absorption as a function of laser frequency and gate voltage V_g for two different sample structures exhibiting radically different ranges of the co-tunneling rate. Fig. 2A shows the 2D absorption map of a QD that is separated from the Fermi sea by a 25 nm GaAs barrier (sample A): each horizontal cut is obtained by scanning the gate voltage for a fixed laser frequency. Red (blue) bars show data obtained by scanning the gate voltage such that the detuning $\Delta\omega = \omega_X - \omega_L$ decreases (increases). We estimate the co-tunneling rate κ_{ct} for this sample at the center of the absorption plateau ($V_g = 200$ mV) to be $1 \cdot 10^6 \text{ s}^{-1}$ from electron spin pumping experiments carried out at $B_{\text{ext}} = 0.3$ T [17]. We observe that the bi-directional dragging effect is strongest in the plateau center and is completely suppressed at the edges ($V_g = 160$ mV and $V_g = 260$ mV).

Figure 2B shows absorption maps for a QD that is separated from the Fermi sea by a 43 nm tunnel barrier (sample B) at two different values of B_{ext} (2 T and 6 T):

each vertical cut is obtained by scanning the laser energy for a fixed gate voltage. The data presented in Fig. 2B is obtained for a narrow range of V_g near the edge of the charging plateau: the large tunnel barrier drastically suppresses the tunnel coupling, such that the highest co-tunneling rate (obtained at the plateau edges) coincides with the lowest rate obtained for sample A [28]. Consequently, bi-directional dragging in sample B extends all the way out to the edge of the charging plateau, while in the plateau center absorption disappears completely due to electron spin pumping into the j_z state [15]. The overall range for dragging is 40 eV (20 eV) for $B_{\text{ext}} = 6$ T ($B_{\text{ext}} = 2$ T) and is symmetrically centered at the bare X transition energy. Further experiments carried out on sample C (not shown) with QDs separated by a 15 nm tunnel barrier from an electron reservoir and exhibiting $\sigma_{\text{ct}} >$ throughout the plateau, did not show dragging effects. These results show that locking of QD resonance to the incident laser energy is possible provided that the co-tunneling rate of the QD electron satisfies $\sigma_{\text{ct}} < 10^8 \text{ s}^{-1}$ [29]. Experiments carried out on QDs in all samples showed that the dragging width increases sub-linearly with B_{ext} beginning at 1 T.

Bi-directional nuclear spin polarization

The disappearance of dragging with increasing co-tunneling rate or vanishing external magnetic field strongly suggest that locking of the QD optical transition to the laser frequency is associated with DNSP. Recent studies carried out with laser fields resonant with the excited state transitions of QDs have shown that the nuclear spin depolarization rate has a strong dependence on the electron spin co-tunneling rate [14]; these experiments also demonstrated that when the QD is neutral, the nuclear spins do not depolarize even on time scales exceeding an hour [18]. To confirm that DNSP indeed plays a key role in our experimental findings, we have carried out experiments to determine the relevant time scales for the buildup and decay of the locking phenomenon in a regime of minimum exchange coupling to the reservoir [30].

Figure 3A presents a set of experiments that reveal the time scales associated with the decay of the DNSP generated during dragging, for the trion transition in sample A at $B_{\text{ext}} = 4.5$ T. The procedure used in these experiments is to first drag the QD trion transition by about 5 meV to the red side of the bare resonance ω_X , and then to abruptly change the detuning between the trion and the laser field by a millisecond voltage ramp. The effect of this ramp is to set a new detuning condition $\omega_X - \omega_L = 4$ meV, which in turn results in an instantaneous loss of the absorption contrast. We observed that after a waiting time on the order of seconds, the initially vanishing absorption strength recovered its maximum value (Fig. 3A, red-coded data). By repeating this experiment for a set of initial detunings ranging from 4 meV to 0, we determined the characteristic exponential time scale for contrast recovery to be 5 sec. When we repeated the same experiment by first dragging the

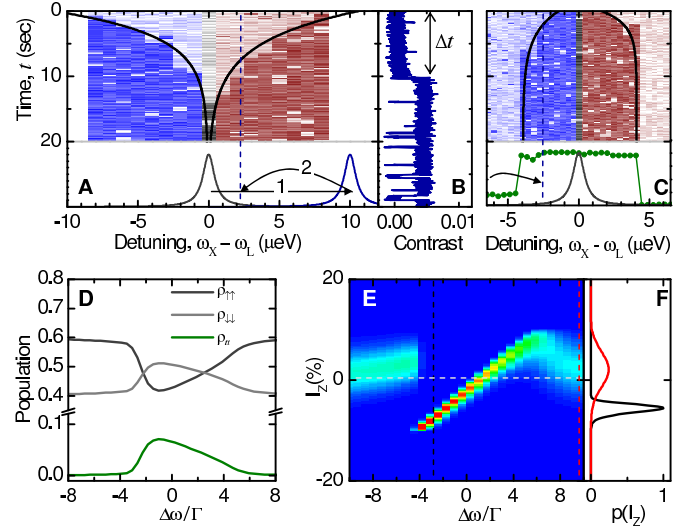


Figure 3: Figure 3 (A) Bi-directional nuclear spin polarization. Decay of nuclear spin polarization determined by measuring the recovery of resonant absorption. The nuclei are dynamically polarized by voltage-controlled dragging up to 10 eV, such that the resulting Overhauser field red (blue) shifts the trion transition, as indicated by arrow 1 in the inset. A millisecond voltage ramp (arrow 2) takes the trion transition into a new detuning condition $\omega_X - \omega_L = 8$ eV and is accompanied by an instantaneous loss of the resonant absorption contrast. The recovery of the full contrast after a time t indicates that the nuclear spin polarization has decayed to reestablish the resonant scattering locking condition. The decay is exponential (solid curves in A) with decay constants $\tau_d = 3.7 \pm 0.7$ sec for blue and 4.9 ± 0.9 sec for red laser detunings, respectively. (B) Time-trace of the on-resonance signal along the dashed line in A, demonstrating the bi-stable behavior of the absorption strength. (C) Buildup of nuclear spin polarization: the nuclear spins are first depolarized by keeping the gate voltage in a region of fast co-tunneling. After depolarization, a finite detuning of the laser from the trion transition is realized within milliseconds by abruptly changing the gate voltage. The buildup time leading to maximum absorption contrast, associated with the build-up of the Overhauser field, is exponential (solid lines with $\tau_b = 3.6 \pm 0.8$ sec for blue, and 2.1 ± 0.7 sec for red laser detunings). (D) Simulation of the quantum dot level populations in steady-state for the experiment described in C. (E) Probability distribution $p(I_z)$ for obtaining a value I_z of the Overhauser field for a detuning range (10 meV). The simulation shows bi-directional nuclear spin polarization as well as a reduction in the Overhauser field variance when the system is locked on to resonance. (F) A vertical line cut from E at zero (large) laser detuning plotted using red (black) dashed line.

trion resonance to the blue side of the bare resonance and monitoring absorption for a final set of detunings satisfying $\omega_X - \omega_L = 4$ meV, we determined a contrast recovery time of $\tau_d = 4$ sec (Fig. 3A, blue-coded data). These results provide information about the decay time of the DNSP that is built up during the dragging process; as DNSP decays in the absence of a resonant laser, the Zeeman shifted trion resonance frequency changes until

it once again reaches resonance condition with the laser field [31]. The DNSP decay times that we determine are in agreement with the values one would extrapolate from earlier experiments where $\tau_{\text{ct}} \sim 10^8 \text{ s}^{-1}$ resulted in DNSP decay times on the order of few milliseconds at $B_{\text{ext}} = 0.2 \text{ T}$ [14]. When we repeated the experiment of Fig. 3 for the neutral QD exciton transition, we observed that the absorption contrast for $|j\rangle_x \rightarrow |j\rangle_L$ always remained zero, indicating that the DNSP decay time was much longer than our measurement time of $\sim 1 \text{ hour}$; this observation is in perfect agreement with earlier experiments [18]. Finally, we remark that the bistable behavior of resonant absorption contrast that is evident in vertical line cuts taken from the data in Fig. 3A (shown in Fig. 3B) is very characteristic of nonlinear nuclear spin dynamics in QDs [10, 11].

Figures 1 and 2 demonstrate that the response of a QD to a given laser detuning strongly depends on how the system reaches that particular detuning. To determine the QD optical response in the absence of such memory effects, we have carried out another set of experiments, where we first set the laser frequency to a large negative detuning with completely negligible excitation of the trion and kept the QD in a parameter regime with a strong co-tunneling rate for several seconds. This procedure allows the QD nuclear spins to thermalize with the lattice, which in turn ensures vanishing nuclear spin polarization. We then abruptly changed the voltage in milliseconds timescale, thereby instantaneously establishing $|j\rangle_x \rightarrow |j\rangle_L$. Subsequently, we observed the time-dependence of the absorption signal at this fixed detuning. Figure 3C shows that for a detuning range of $3 \text{ meV} < |j\rangle_x \rightarrow |j\rangle_L$, the absorption strength grows from zero to its maximum value on a timescale of a few seconds while within $|j\rangle_x \rightarrow |j\rangle_L$ the on-resonance condition is established on a timescale below the temporal resolution limit of a few milliseconds in our experiment. Even though the frequency range over which the QD is able to lock on to the laser field is identical for red and blue detunings, the absorption recovery time is a factor of 2 slower for a laser that is tuned to the blue side of the bare trion resonance. We also note that the frequency range over which full absorption is recovered in these fixed laser frequency dragging experiments (green curve in Fig. 1C and Fig. 3C) is narrower than that of dynamical dragging bandwidth obtained by tuning the laser across the resonance (red and blue curves in Fig. 1C).

Perhaps the most unexpected feature of our experiments is the remarkably symmetric dragging effect that indicates bi-directional DNSP; this observation is in stark contrast with recent experiments which demonstrated unidirectional dragging of the electron (microwave) spin resonance and the bi-stability of the coupled QD electron-nuclei system [19]. These results, obtained concurrently, could be understood as arising from a dominant nuclear spin pumping process that is a nonlinear function of the degree of DNSP and competes with the nuclear spin depolarization processes [20, 21].

We understand the bi-directionality of DNSP by considering that the optical excitation of the QD blue-trion transition (Fig. 1A) induces two competing nuclear spin pumping processes that try to polarize QD nuclear spins in two opposite directions and that have a different functional dependence on the laser detuning $\delta = E_x - E_L$; here E_x is the QD blue trion transition energy shifted by DNSP. As we argue below, the reverse-O verhauser process [20] that polarizes the nuclear spins along $+\hat{z}$ direction depends linearly on the absorption rate $W_{\text{abs}} = \Gamma_L^2 = (\Gamma^2 + \delta^2)$ from the $|j\rangle_z$ state and dominates for large $|j|$ [32]. In contrast, the O verhauser process that polarizes the nuclear spins along $-\hat{z}$ scales as W_{abs}^2 and determines the direction of DNSP for small values of $|j|$ [33]. The two opposing processes balance each other out at a finite red or blue detuning [20]. The red detuning ($E_x > E_L$) where the net polarization rate vanishes is a stable point of the coupled system: tuning the laser closer to (away from) resonance would lead to an enhanced O verhauser (reverse-O verhauser) process which would ensure that the trion resonance is blue (red) shifted until the stable point is once again reached. In addition to the O verhauser and reverse-O verhauser channels, there are pure DNSP decay processes that are induced either by exchange interactions with the Fermi sea or by electron-phonon interactions.

The interplay between the two polarization channels ensures that DNSP in either direction can be attained [34]; the maximum DNSP that can be achieved is in turn determined by the co-tunneling or phonon assisted DNSP decay processes. To gain further insight into this interplay, we have solved the master equation describing the evolution of the coupled electron-nuclear spin system in steady-state: to obtain a tractable master equation for $N \sim 1000$ spins, we have modeled the nuclear spin system in the Dicke basis of collective spin states $|j\rangle_z$ having a total angular momentum I ($0 \leq I \leq N/2$) and that couple to the QD electron via hyperfine interaction. States belonging to different I but having identical spin projection I_z along B_{ext} are assumed to be coupled weakly by incoherent jump processes [35]. The overall contribution of each I to the coupled dynamics is weighted by the number $D(I)$ of allowed permutation group quantum numbers associated with that total angular momentum [22]. The master equation is obtained by first applying a Schrieffer-Wolff transformation that eliminates the off-diagonal terms of the hyperfine interaction, and then tracing over the electron-spin and radiation field reservoirs in the Born-Markov limit.

Figure 3D shows the steady state electron spin and trion populations evaluated for a range of fixed laser detunings using this procedure. The trion population as a function of the laser detuning is a direct measure of the absorption strength that we experimentally determined in Fig. 3C: we observe that our model reproduces the broadened absorption profile but does not capture the sharp change in the absorption strength that we observe experimentally. This discrepancy is most likely due to

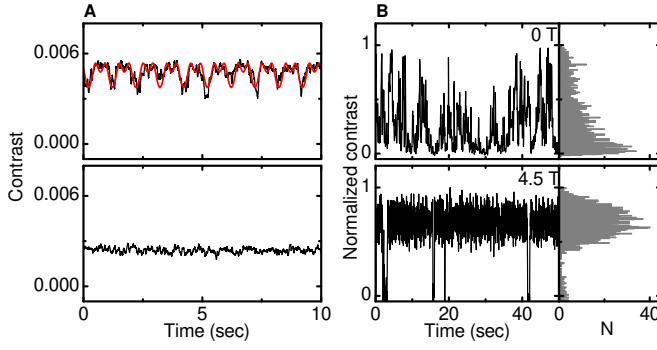


Figure 4: Figure 4 (A) Suppression of fluctuations in quantum dot resonance frequency. Suppression of the fluctuations in the resonant absorption signal when the dragging condition is satisfied in sample B. Upper panel: the measured absorption contrast as a function of time at a fixed laser at $B_{\text{ext}} = 0$ T in the presence of a 1 Hz sinusoidal gate voltage modulation. The modulation amplitude corresponds to a shift of the trion transition by ≈ 2 starting from exact resonance condition. Lower panel: the corresponding time dependent fixed laser frequency absorption contrast at $B_{\text{ext}} = 4$ T when dragging is present. The signal shows full compensation of the externally induced detuning modulation. (B) The fluctuations in the resonant absorption signal observed for the quantum dot in Sample A at 0 T (upper panel) are suppressed in the presence of dragging at 4.5 T (lower panel); the data in both panels of (B) are normalized to peak absorption contrast obtained at the corresponding magnetic field.

the fact that our calculations give the steady-state values which may be practically impossible to observe experimentally. Fig. 3E shows the probability distribution $p(I_z) = \text{Tr}[\rho I_z] / \text{Tr}[\rho]$ for obtaining a specific value I_z of the Overhauser field, evaluated for the same range of parameters used in Fig. 3C: these results demonstrate that the bi-directional dragging indeed originates from a bi-directional DNSP. Perhaps more important is the fact that $p(I_z)$ reveals an impressive reduction in the Overhauser field variance by more than a factor of 5, when dragging is present (Fig. 3F).

Suppression of fluctuations in quantum dot transition energy

The experiments depicted in Figs. 1–3 as well as the numerical results shown in Fig. 3D demonstrate the existence of a feedback mechanism that polarizes the necessary number of nuclear spins needed to shift the transition energy in a way to maintain resonance with the excitation laser. Consequently, fluctuations in the QD transition energy that would normally lead to a fluctuating absorption signal should be suppressed by such a compensation mechanism provided that the fluctuations occur within the effective feedback bandwidth. Figure 4A shows the time-dependence of the absorption signal for $B_{\text{ext}} = 0$ T and $B_{\text{ext}} = 4$ T for sample B in the presence of external modulation of the trion resonance energy. The upper panel shows a time record of the on-resonance signal for $B_{\text{ext}} = 0$ T with 10 millisecond time resolution

and in the presence of a controlled disturbance of the trion transition energy. This is achieved by introducing a 1-Hz sine modulation on the gate voltage with a peak-to-peak voltage amplitude corresponding to ≈ 2 via Stark shift. The $B_{\text{ext}} = 0$ T signal on resonance clearly reproduces this modulation as the transition goes in and out of resonance with the laser consistent with the expected signal drop. However, $B_{\text{ext}} = 4$ T on-resonance signal shows complete suppression of this external disturbance of the transition energy (lower panel). The same experiment repeated for higher frequencies show that suppression works at least up to 10 Hz detuning the relevant bandwidth for Overhauser field dynamics for this particular QD and gate voltage. When the disturbance is in the form of a square wave modulation of peak-to-peak amplitude less than ≈ 2 , suppression is still present, while beyond ≈ 2 modulation, no suppression can be seen regardless of modulation frequency. This is consistent with the slow timescale of DNSP buildup of sample B in comparison to the abrupt jump of the transition under square wave modulation.

Even in the absence of an external perturbation, most QDs exhibit time-dependent fluctuations in I_x [2]: these fluctuations could arise either from the electromagnetic environment of the QD or fluctuating nuclear Overhauser field. Figure 4B (upper panel) shows a typical time record of the resonant absorption signal of sample A QD together with the corresponding distribution function for I_L : in contrast to the sample B QD studied in Fig. 4A, we observe up to 100% fluctuations in the resonant absorption signal, which is in turn a factor of 3 larger than our noise floor. In contrast, for $B_{\text{ext}} = 4.5$ T (Fig. 4B lower panel), we find that the fluctuations in the absorption signal are reduced to the noise floor. The absorption signal occasionally drops to zero, indicating bistability in the response of the coupled electron-nuclei system to the resonant laser field. The frequency of jumps in absorption strength depends strongly on the system parameters; in particular sample B QD practically never showed jumps during the observation period exceeding 10 sec.

Having demonstrated that the locking of the QD resonance to the incident laser frequency via selective DNSP strongly damps out the fluctuations in electronic transition energy, we address the possibility of suppressing the time-dependent fluctuations in the nuclear Overhauser field [12, 23]. Given that the effective Zeeman shift associated with the rms Overhauser field of the QD nuclei B_{nuc} is comparable to the spontaneous emission rate, we would expect that the fluctuations in the Overhauser field would lead to sizable fluctuations of the resonant absorption signal on time-scales that are characteristic for the Overhauser field (few seconds). Since we lack controlled experiments exclusively demonstrating the role of the Overhauser field fluctuations on the absorption signal, we could only claim that the experiments depicted in Fig. 4 provide an indirect evidence for a suppression of nuclear Overhauser field fluctuations that is predicted

by our theoretical model (Fig. 3E and F).

We emphasize that a narrowing of the Overhauser field variance would have remarkable consequences for quantum information processing based on spins. In particular, a major limitation for experiments detecting spin coherence in QDs is the random, quasi-static Overhauser field that leads to an inhomogeneous broadening of the spin transition with a short T_2 time [3]. Suppression of the long-timescale Overhauser field fluctuations by laser dragging may be used to ensure that the time/ensemble averaged spin coherence measurements yield a dephasing time that is limited only by the fundamental spin decoherence processes [24, 25, 26]. While replacing the more traditional spin-echo techniques with laser dragging

would represent a practical advantage for optical experiments, a more intriguing possibility would be the slowing down of nuclear spin dynamics by a combination of large inhomogeneous quadrupolar shifts [18] and dragging, which would in turn prolong the inherent electron spin coherence time.

Acknowledgments

We thank Hakan Tureci, Jake Taylor, Geza Giedke, Mark Rudner and Lev Levitov for discussions.

-
- [1] M ichler, P. et al. A Quantum Dot Single-Photon Turnstile Device. *Science*, 290, 2282 (2000).
 - [2] H ogele, A. et al. Voltage-controlled optics of a quantum dot. *Phys. Rev. Lett.* 93, 217401 (2004).
 - [3] Petta, J. R. et al. Coherent Manipulation of Coupled Electron Spins in Semiconductor Quantum Dots. *Science* 309, 2180 (2005).
 - [4] Braun, P. F. et al. Direct Observation of the Electron Spin Relaxation Induced by Nuclei in Quantum Dot. *Phys. Rev. Lett.* 94, 116601 (2005).
 - [5] Khaetskii, A., Loss, D. & Glazman, L. Electron Spin Decoherence in Quantum Dots due to Interaction with Nuclei. *Phys. Rev. Lett.* 88, 186802 (2002).
 - [6] Gammon, D. et al. Electron and Nuclear Spin Interactions in the Optical Spectra of Single GaAs Quantum Dots. *Phys. Rev. Lett.* 86, 5176 (2001).
 - [7] Ebble, B. et al. Dynamic nuclear polarization of a single charge-tunable InAs/GaAs quantum dot. *Phys. Rev. B* 74, 081306 (2006).
 - [8] Koppens, F. H. L. et al. Driven coherent oscillations of a single electron spin in a quantum dot. *Nature* 442, 766 (2006).
 - [9] Lai, C. W., M aletinsky, P., Badolato, A. & Imamoglu, A. Knight-Field-Enabled Nuclear Spin Polarization in Single Quantum Dots. *Phys. Rev. Lett.* 96, 167403 (2006).
 - [10] M aletinsky, P. et al. Nonlinear dynamics of quantum dot nuclear spins. *Phys. Rev. B* 75, 035409 (2007).
 - [11] Tartakovskii, A. et al. Nuclear Spin Switch in Semiconductor Quantum Dots. *Phys. Rev. Lett.* 98, 026806 (2007).
 - [12] Reilly, D. et al. Suppressing Spin Qubit Dephasing by Nuclear State Preparation. *Science* 321, 718 (2008).
 - [13] Smith, J. M. et al. Voltage Control of the Spin Dynamics of an Exciton in a Semiconductor Quantum Dot. *Phys. Rev. Lett.* 94, 197402 (2005).
 - [14] M aletinsky, P. et al. Dynamics of Quantum Dot Nuclear Spin Polarization Controlled by a Single Electron. *Phys. Rev. Lett.* 99, 056804 (2007).
 - [15] A tature, M. et al. Quantum-Dot Spin-State Preparation with Near-Unity Fidelity. *Science* 312, 551 (2006).
 - [16] Bayer, M. et al. Electron and Hole Factors and Exchange Interaction from Studies of the Exciton Fine Structure in $\text{In}_{0.60}\text{Ga}_{0.40}\text{As}$ Quantum Dots. *Phys. Rev. Lett.* 82, 1748 (1999).
 - [17] Dreiser, J. et al. Optical Investigations of Quantum Dot Spin Dynamics as a Function of External Electric and Magnetic Fields. *Phys. Rev. B* 77, 075317 (2008).
 - [18] M aletinsky, P., Kroner, M. & Imamoglu, A. Breakdown of the nuclear spin temperature approach in quantum dot demagnetization experiments. *arXiv:0901.2289* (to appear in *Nature Physics*).
 - [19] Vink, I. T. et al. Locking electron spins into magnetic resonance by electron-nuclear feedback. *arXiv:0902.2659*.
 - [20] Rudner, M. & Levitov, L. Electrically Driven Reverse Overhauser Pumping of Nuclear Spins in Quantum Dots. *Phys. Rev. Lett.* 99, 246602 (2007).
 - [21] Danon, J. & Nazarov, Y. V. Nuclear tuning and detuning of the electron spin resonance in a quantum dot: theoretical consideration. *Phys. Rev. Lett.* 100, 056603 (2008).
 - [22] Taylor, J. M., Imamoglu, A. & Lukin, M. D. Controlling a Mesoscopic Spin Environment by Quantum Bit Manipulation. *Phys. Rev. Lett.* 91, 246802 (2003).
 - [23] Greilich, A. et al. Mode Locking of Electron Spin Coherences in Singly Charged Quantum Dots. *Science* 313, 341 (2006).
 - [24] Coish, W. A. & Loss, D. Hyperfine interaction in a quantum dot: Non-Markovian electron spin dynamics. *Phys. Rev. B* 70, 195340 (2004).
 - [25] Taylor, J. M. et al. Relaxation, dephasing, and quantum control of electron spins in double quantum dots. *Phys. Rev. B* 76, 035315 (2007).
 - [26] Cywinski, L., W itzel, W. M. & Das Sarma, S. Electron Spin Dephasing due to Hyperfine Interactions with a Nuclear Spin Bath. *Phys. Rev. Lett.* 102, 057601 (2009).
 - [27] Bidirectional DNSP is also observed when the red-trion or the red-Zeeman bright exciton transitions are driven by a resonant laser field; in contrast to the blue-trion (Fig. 1C) and high-energy bright exciton (Fig. 1D) transitions, the forward and backward scans in this case are highly asymmetric.
 - [28] The plateau middle sees a further 6 orders of magnitude reduction in the co-tunneling rate.
 - [29] We observed that the neutral exciton transition (that is not limited by electron spin pumping) of sample B QD exhibits dragging even at the center of the plateau where we expect $\tau_{\text{et}} \sim 1 \text{ s}^{-1}$. This observation suggests that dragging of the QD resonances takes place even for QDs that are completely isolated from a back contact.

- [30] A direct proof of D N S P using depolarization by resonant radio frequency magnetic fields does not appear to be possible in self-assembled Q D s due to large inhomogeneous quadrupolar fields [18].
- [31] Since the presence of a laser field that is detuned by less than 2π would speed up the recovery of resonant absorption (see Fig. 3C), the timescales we obtain in this experiment could be regarded as an upper bound on the nuclear spin depolarization rate.
- [32] The reverse O verhauser process is associated with hyperfine assisted spin- ip Raman scattering and is the resonant analog of the optical pumping effect that the early D N S P experiments [6, 7] were based on.
- [33] The O verhauser process is effected by optical pumping of the electron spin via heavy-light-hole mixing induced spontaneous Raman scattering, together with a resonant-absorption induced spin dephasing mechanism that is proportional to W_{abs} . Since the excess spin population in state $j \neq i$ is also proportional to W_{abs} , the overall spin-dephasing-induced O verhauser processes depend on W_{abs}^2 .
- [34] The unexpected dragging observed on the Q D X^0 transition could also be understood as arising from a similar competition between detuning dependent O verhauser and reverse-O verhauser processes. The asymmetry in bidirectional dragging we observed in the red trion transition could be due to the fact that the (phonon mediated) relaxation is reduced at low temperatures for the low energy trion state.
- [35] This coupling would have been identically zero, if the hyperfine coupling to each nuclei had been identical.